The Robot-Pedestrian Influence Dataset for Learning Distinct Social Navigation Forces

Subham Agrawal Nico Ostermann-Myrau Nils Dengler Maren Bennewitz

***Abstract*— Existing research lacks comprehensive datasets that capture the full range of pedestrian behaviors, e.g., including avoidance, neutrality, and attraction in the presence of robots. In this paper, we present a novel dataset capturing pedestrian behavior in the presence of robots under varying conditions, enabling better prediction of responses like avoidance or attraction. Leveraging this, we introduce the Neural Social Robot Force Model (NSRFM), which outperforms baselines in predicting real-world pedestrian trajectories and supports the development of socially-aware robot navigation.**

I. Introduction

Understanding and modeling pedestrian behavior in shared environments with robots is crucial to ensure effective and safe navigation as well as seamless human-robot interaction. With the increasing presence of robots in public spaces such as shopping malls [1], sidewalks [2], [3], hospitals [4], it becomes essential to develop robust navigation systems capable of moving among humans without causing disruptions. This challenge is intensified by the bidirectional interaction between humans and robots, where pedestrians influence robot behavior, and vice versa. Despite significant advances in autonomous navigation, current systems often struggle to adapt to human behaviors such as context-dependent reactions to robots [2], [3], leading to suboptimal performance in pedestrian-rich environments.

Therefore, effective social navigation for robots requires a well-defined representation of pedestrian behavior. The key challenge lies in accurately modeling how pedestrians respond to robots, as many existing approaches either focus on reactive robot control or rely on overly simplistic pedestrian models. Consequently, they often fail to capture the nuanced, context-dependent nature of human behavior [5], as contrary to common assumptions, pedestrians do not exclusively avoid robots. As illustrated in Fig. 1, their responses may vary and can include behaviors such as avoiding, ignoring, or even approaching the robot driven by curiosity [6]. Accurately modeling, detecting, and predicting these diverse behaviors is crucial for developing navigation strategies that enable robots to integrate seamlessly into human environments.

Learning these pedestrian behaviors and generating effective robot navigation policies requires high-quality datasets. However, existing trajectory datasets [7]–[9] do not explicitly capture or annotate pedestrian reactions to the robot in the scene, making it difficult to learn pedestrian behaviors

All authors are with the Humanoid Robots Lab, University of Bonn, Germany. M. Bennewitz, S. Agrawal, and N. Dengler are additionally with the Lamarr Institute for Machine Learning and Artificial Intelligence and the Center for Robotics, Bonn, Germany. This work has been partially funded by the BMBF, within the Robotics Institute Germany, grant No. 16ME0999.

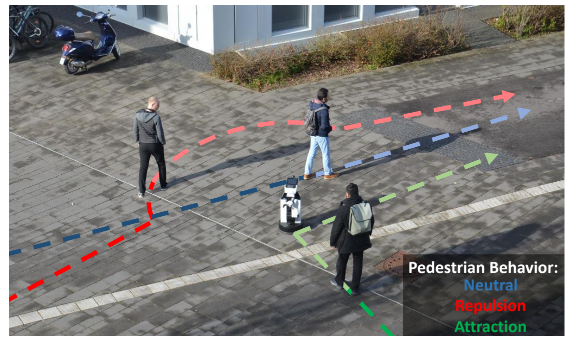

Fig. 1: Example scenario of a robot influencing the trajectories of nearby pedestrians, leading them to show one of three distinct behaviors: avoidance, neutrality, or attraction.

effectively. Additionally, existing evaluation frameworks often lack the ability to comprehensively model diverse pedestrian behaviors and assess robot navigation policies beyond standard metrics, such as arrival rate, collision rate, and time to goal. A more nuanced approach is needed to capture the robot's influence on pedestrian trajectories, including deviations from the shortest path [5].

In this paper, we propose to overcome these limitations through two key contributions: (i) a real-world pedestrian dataset capturing diverse human-robot interactions and (ii) a neural social robot force model (NSRFM) that enhances the traditional social force model (SFM) [10] for pedestrian trajectory prediction. Our dataset captures pedestrian trajectories under three conditions—no robot, a stationary robot, and a moving robot—highlighting the distinct behaviors of *avoidance*, *neutrality*, and *attraction* potentially observed in each scenario. Using the pedestrian trajectories of our dataset, we train five individual networks, each mimicking a distinct force of the NSRFM, to predict diverse pedestrian behaviors. This approach allows for a better prediction of trajectories influenced by robots compared to the original SFM. Our experimental evaluation demonstrates that the NSRFM outperforms the traditional SFM and variations in predicting pedestrian trajectories, effectively capturing diverse human-robot interactions. Together, these elements contribute to the development of diverse social robot navigation strategies.

II. Robot-Pedestrian Influence Dataset

Since existing large-scale datasets lack explicite annotations of pedestrian-robot responses, we collected our own robot-pedestrian influence (RPI) dataset. It is designed to capture diverse pedestrian behaviors and enable the learning of the various forces that will be incorporated in our novel Neural Social Robot Force Model (NSRFM, see Sec. III). We now

(a) Environment 1 (b) Environment 2

Fig. 2: Outdoor environments used for data collection. (a) A pathway crossing with two office building entries. (b) A larger university campus open space.

describe the key aspects of our data collection process.

*1) **Overview**:* We collected data in two outdoor environments (see Fig. 2) with naturally present pedestrian entry and exit points. Environment 1 is a $50\,m \times 20\,m$ crossing, while Environment 2 corresponds to a $50\,m \times 60\,m$ open space. We used a bird's-eye view camera, as in Fig. 2, operating at $15\ Hz$ to capture the pedestrian trajectories and robot positions. The data collection was conducted for two weeks during periods when both individual and group trajectories were likely to occur, ensuring representation of these modalities in the dataset. In total, we recorded 18,669 trajectories across 142 hours of data in the two environments, with $16.45\ \%$ of the trajectories including pedestrian-robot responses. The average velocity of the pedestrians in our dataset is $1.51 m/s$.

*2) **Detection and Tracking**:* We detected and tracked pedestrians in real-time using a YOLOv11 [11] model. Their positions were projected onto the ground plane and converted into 2D real-world coordinates, ensuring data privacy by avoiding the storage of any identifiable information.

*3) **Trajectory Filtering**:* Due to factors such as pedestrians standing still for long periods, abruptly changing direction, or moving unpredictably while talking on the phone, we found trajectories that were unusable for model training. Hence, we applied filters to remove all trajectories that were shorter than 3.5 m, exceeded a speed of $2.7\ \mathrm{m/s}$ (running or cycling), or contained loops.

*4) **Robots**:* For data collection, we used three different robots, Toyota's Human Support Robot (HSR), Neobotix's MPO700, and Unitree's Go1 to study pedestrian interactions. HSR is a mobile manipulator designed for human interaction tasks, MPO700 an industrial mobile manipulator platform, and Go1 a quadrupedal robot. Their varying sizes and mobility types allowed us to analyze diverse pedestrian responses in different scenarios.

*5) **Interaction Types**:* To capture diverse pedestrian-robot interactions, we considered three distinct scenarios:

- **Pedestrians Only (PD):** No robot was present, and only pedestrian trajectories were tracked. This scenario provides baseline data for modeling fundamental pedestrian behaviors, including attraction toward a goal (f_a), repulsion from other pedestrians (f_p), repulsion from obstacles (f_o), and group dynamics (f_{gr}) in an extension of the Social Force Model [12].
- **Pedestrians with a Stationary Robot (PD-SR):** One of the three robots was placed at a fixed location while pedestrian movements were recorded to analyze how individuals react to a stationary robot. This setup provides valuable data for modeling robot-induced forces (f_{rs}) based on different robot types. The results, shown in Tab. I, indicate that pedestrian responses varied depending on the robot type present. Overall, the most attraction was shown towards the GO1, while our industrial robot MPO700 showed the least attraction behavior. These findings suggest that different robot designs cause distinct social responses, which can inform the development of socially aware navigation strategies.
- **Pedestrians with a Moving Robot (PD-MR):** In the Scenario, the GO1 was teleoperated around a central location while pedestrian trajectories were tracked. This scenario enables comparisons of pedestrian responses to stationary versus moving robots and provides data to model robot-related forces based on the robot's state of motion (f_{rm}). We observed that the moving robot had the highest attraction rate.

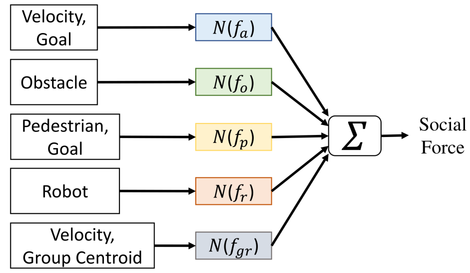

Fig. 3: Structure of our new NSRFM for pedestrian trajectory prediction. The input to NSRFM include pedestrian velocity, goal direction, distance and direction to other pedestrians, distance and direction to the robot, and direction to the group centroid. These inputs are provided to the 5 different networks and the final outputs are combined to get the resulting social force acting on the pedestrian.

Robot Type	Attraction (%)	Avoidance (%)	Avg. Distance (m)
HSR (Stationary)	4.39	27.17	3.05
MPO700 (Stationary)	1.6	33.95	3.26
Go1 (Stationary)	7.82	26.39	3.24
Go1 (Moving)	7.96	26.1	3.41

TABLE I: Pedestrian Responses to Stationary and Moving Robots in terms of attraction, avoidance, and average distance maintained.

Our dataset consists of $15,461$ trajectories for the PD case, $2,948$ trajectories (1090 for **HSR**, 837 for **MPO700** and 1021 for **GO1**) for PD-SR, and 260 trajectories for the PD-MR, providing a diverse range of pedestrian responses to robots across different scenarios.

*6) **Data Structure**:* We store the data in the following format:

- **Frame Number**: The sequential index and timestamp of the stored frame.
- **Pedestrian ID**: A unique identifier for each individual pedestrian. Note that pedestrians who leave and re-enter the observed area are assigned new identifiers and treated as distinct individuals.
- **x and y Position**: The pedestrian's 2D position (in meters) relative to the scene's origin.
- **Distance Increment**: The change in position (in meters) between two consecutive time frames, used to compute velocities.

- **Robot Presence**: A boolean flag indicating whether a robot is present in the scene.
- **Robot Type**: A classification label indicating the used robot type.
- **Robot Influence**: A classification label indicating the pedestrian's response with the robot, categorized as *attractive*, *repulsive*, or *neutral*, if a robot is present in the scene.

III. Neural Social Robot Force Model (NSRFM)

The traditional Social Force Model (SFM) [10] defines pedestrian motion as a result of attractive and repulsive forces, including a goal-directed attraction force (f_a), repulsion from other pedestrians (f_p), and repulsion from obstacles (f_o):

$$F = f_a + f_o + f_p \tag{1}$$

A. Extension of the Traditional Social Force Model

In previous work [13], we demonstrated the need to augment the SFM with additional forces, such as a robot force, since the traditional SFM fails to capture the nuanced behaviors exhibited when pedestrians encounter robots. Additionally, we found that group forces significantly impact pedestrian behavior near robots, as they can influence an individual to move closer or farther away, independent of their intrinsic behavior. To address these complexities, we enhance the traditional SFM by an additional robot force (f_r) to model pedestrian-robot responses [13], [14] and a group force (f_{gr}) [12] to capture these social influences on human trajectories. Therefore, Eq. 1 extends to:

$$F = f_a + f_o + f_p + f_{gr} + f_r \tag{2}$$

Note that the additional robot force only models the repulsion behavior of pedestrians from a robot. However, our observations from the RPI dataset revealed that repulsive behavior towards a robot is not the only response, as pedestrians may also show attraction or neutrality, which has to be taken into account. Therefore, we define neutral behavior as treating the robot as an obstacle, without any individual response or force directed toward it. Additionally, we observed that the repulsive effect of a moving robot on pedestrians is similar to, but stronger than that of a stationary robot, i.e., $f_{rm} > f_{rs}$. Therefore, to simplify learning the repulsive force, we assume $f_r = f_{rm}$. Similarly, we noticed variations in repulsion behavior depending on the type of robot used. However, in this paper, we use the maximum repulsion across the different robot types for further calculations.

B. Learning the Parameters of the NSFRM

The original SFM uses mathematical formulas to represent its individual forces, requiring extensive fine-tuning and expert input for parameter optimization [12]. Inspired by Zhang *et al.* [15] and Hossain *et al.* [12], we replace these hand-crafted formulas with neural network-based models.

Our proposed NSRFM learns force parameters directly from real-world data, eliminating the need for extensive manual tuning. To learn the individual forces of the NSRFM, we employ five separate networks to compute the force factors that drive pedestrian motion, as shown in Fig. 3. Each model captures a distinct force component within the NSRFM, while their outputs are summed to compute the final pedestrian force which updates their velocity. To counter bias in the RPI dataset, we limit the pedestrian speed to $1.34\ \mathrm{m/s}$ as found across literature [16], [17].

*1) **Goal Attraction,** $N(f_a)$:* A twin-branched multi-layer perceptron (MLP) that predicts goal-directed forces. One branch processes the pedestrian's velocity, while the other uses goal direction. Trained on straight-line trajectories, it ensures accurate goal-seeking behavior.

*2) **Obstacle Repulsion,** $N(f_o)$:* A two-stage MLP that takes the distance and unit direction vector to obstacles as input, outputting repulsion forces in the x and y directions. Trained on pedestrian trajectories that demonstrate direct obstacle avoidance.

*3) **Pedestrian Repulsion,** $N(f_p)$:* Similar to $N(f_a)$ but incorporates inputs for pedestrian distance and direction. Due to the anisotropy of human perception and attention, it filters for individuals outside the pedestrian's field of view and is trained on real and synthetic avoidance trajectories.

*4) **Robot Repulsion,** $N(f_r)$:* Similar in structure to the $N(f_o)$, this model predicts pedestrian repulsion from robots based on distance and direction. It is trained on trajectories where pedestrians show evasive behavior near robots.

*5) **Group Cohesion,** $N(f_{gr})$:* A twin-branched model that maintains pedestrian proximity to a group. One branch processes velocity in the direction of goal, while the other uses the direction to the group centroid, outputting an attraction force toward the group.

C. Behavior Detection

For dataset labeling it is essential to classify distinct human behaviors in response to the robot's presence in the scene. To achieve this, we introduce a heuristic-based detection approach. At each time step, we analyze the pedestrian's heading and define an attraction cone with an angle range of $[-\epsilon, \epsilon]$. If the pedestrian is within the robot's social zone [18] of influence ($3\ \mathrm{m}$) and the robot's position falls within the cone, we classify the pedestrian's behavior as attraction toward the robot. Conversely, if the robot's position is outside the cone and the pedestrian's current heading deviates away from the robot compared to their past heading by more than a threshold factor ϕ, the behavior is classified as repulsion. If neither condition is met, the behavior is classified as neutral. Fig. 4 illustrates example trajectories for each behavior, highlighting the differences in pedestrian movement patterns.

IV. Experimental Evaluation

In our experimental evaluation, we first compare our RPI dataset against the ETH [19] and JRDB [7] datasets by comparing the number of pedestrian trajectories recorded both in the presence and absence of a robot. Then, we validate our learned NSRFM model by comparing its trajectory predictions against ground truth data, a tuned SFM [10], and the SRFM [13] baseline. In addition, our supplemental

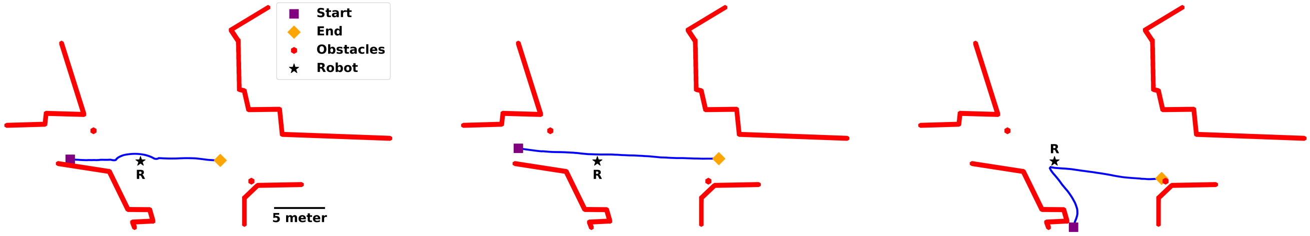

(a) Avoidance behavior (b) Neutral behavior (c) Attraction behavior

Fig. 4: Distinct pedestrian behaviors when close to robots taken from our RPI dataset: (a) The pedestrian clearly avoids the static robot (star) while walking toward their goal. (b) The pedestrian walks close to the robot without any noticeable change in trajectory direction. (c) The pedestrian deviates from their original path to approach the robot before resuming their goal-directed movement.

Dataset	Trajectories	HRI Trajectories	Percentage
ETH [8]	750	0	0 %
JRDB [7]	1,786	28	1.57 %
RPI (Ours)	**18,669**	**3,071**	**16.45 %**

TABLE II: Comparison of common datasets with robot presence in terms of number of trajectories with and without human-robot interaction. Our dataset shows the highest percentage of trajectories where the human reacts to the presence of the robot in the scene.

video[1] shows examples of recorded trajectories and a real robot trained to respond to the distinct pedestrian behaviors shown in this paper.

A. Dataset Comparison

We compare the datasets in terms of total trajectories, robot-influenced trajectories (RIT), and the percentage of RITs in the whole dataset (see Tab II). The ETH dataset is a benchmark standard for pedestrian trajectory prediction, containing 750 trajectories. However, it does not include human-robot interactions, making it unsuitable for evaluating pedestrian responses to robots.

The JRDB dataset includes 1,786 total trajectories, of which 28 involve RITs. Unlike other datasets, JRDB provides both indoor and outdoor scenes and offers readily available pedestrian data relative to the robot's position, eliminating the need for extensive preprocessing (e.g., extracting pedestrian information from LiDAR or other sensor data).

In contrast, our RPI dataset provides a significantly larger sample size, with 18,669 total trajectories, including 3,071 RITs. With the highest RIT percentage of 16.45%, this makes it the most comprehensive dataset for studying pedestrian responses to robots in real-world environments. The greater proportion of RITs allows for more robust evaluation of models incorporating robot forces fr.

These findings highlight the RPI dataset's advantage in modeling pedestrian behavior in the presence of robots, making it a valuable benchmark for developing socially aware navigation systems.

B. Performance Comparison of SFM Variants

We evaluate different variations of the Social Force Model (SFM) using the Average Displacement Error (ADE) on three datasets: ETH, JRDB, and RPI. ADE measures the mean deviation between predicted and actual pedestrian trajectories, with lower values indicating better predictive accuracy.

Table III compares our NSRFM with and without group force and robot force effects, alongside the optimization-based

[1] https://www.hrl.uni-bonn.de/publications/rpi.mp4

Model	**Average Displacement Error (ADE) ↓**		
	ETH	JRDB	RPI (Ours)
NSRFM (with group force)	**0.474**	**0.217**	**0.744**
NSRFM (without group force)	0.506	**0.217**	**0.744**
NSRFM (without robot force)	0.506	0.38	0.753
SRFM [13]	0.616	0.336	1.117
SFM [10]	0.616	0.412	1.118

TABLE III: Comparison of different variations of the SFM in terms of Average Displacement Error (ADE) in meters. The results demonstrate that our NSRFM achieves the lowest ADE across all datasets, highlighting the effectiveness of incorporating robot forces, group forces, and learning-based approaches for force prediction. Our dataset shows higher ADEs compared to others due to predicting over longer trajectory lengths (139 frames in RPI compared to 18.1 in ETH and 58.67 in JRDB).

SRFM [13] and the classical SFM [10]. Note, that the JRDB dataset includes no group dynamics information, meaning that incorporating group force f_{gr} has no effect. Similarly, ETH does not include robot presence, leading to identical results for SRFM and SFM since robot force fr is their only distinguishing factor.

The results show that NSRFM consistently achieves the lowest ADE across all datasets, demonstrating good predictive capability. Additionally, incorporating f_{gr} further reduces ADE in datasets where group information is available, highlighting the importance of group dynamics. Furthermore, the use of robot force f_r in SRFM improves performance over classical SFM, while learning-based optimization of the forces in NSRFM further enhances accuracy.

These findings confirm that group forces, robot forces, and learning-based approaches significantly improve trajectory prediction compared to traditional manually tuned models.

V. Conclusion

In this paper, we presented a novel dataset and modeling approach for improved pedestrian behavior prediction in human-robot environments. Our Robot-Pedestrian Influence (RPI) dataset captures pedestrian trajectories without robots, with a stationary robot, and with a moving robot, highlighting pedestrian avoidance, neutrality, and attraction behaviors throughout these cases. Unlike existing datasets, RPI explicitly annotates pedestrian responses to robots.

To model the different behaviors, we propose the Neural Social Robot Force Model (NSRFM), an extension of the traditional Social Force Model (SFM). By integrating neural network-based forces for pedestrian goals, obstacles, group dynamics, and robot influence, NSRFM greatly improves the trajectory prediction as our experimental results demonstrate.

References

[1] M. Niemelä, P. Heikkilä, H. Lammi, and V. Oksman, "A social robot in a shopping mall: studies on acceptance and stakeholder expectations," *Social robots: Technological, societal and ethical aspects of human-robot interaction*, 2019.

[2] H. Han, F. M. Li, N. Martelaro, D. Byrne, and S. E. Fox, "The robot in our path: Investigating the perceptions of people with motor disabilities on navigating public space alongside sidewalk robots," in *Proc. of the ACM SIGACCESS Intl. Conf. on Computers and Accessibility (ASSETS)*, 2023.

[3] D. Weinberg, H. Dwyer, S. E. Fox, and N. Martelaro, "Sharing the sidewalk: Observing delivery robot interactions with pedestrians during a pilot in Pittsburgh, PA," *Multimodal Technologies and Interaction*, 2023.

[4] M. Kyrarini, F. Lygerakis, A. Rajavenkatanarayanan, C. Sevastopoulos, H. R. Nambiappan, K. K. Chaitanya, A. R. Babu, J. Mathew, and F. Makedon, "A survey of robots in healthcare," *Technologies*, 2021.

[5] C. Mavrogiannis, F. Baldini, A. Wang, D. Zhao, P. Trautman, A. Steinfeld, and J. Oh, "Core challenges of social robot navigation: A survey," *ACM Trans. on Human-Robot Interaction*, 2023.

[6] F. Babel, J. Kraus, and M. Baumann, "Findings from a qualitative field study with an autonomous robot in public: exploration of user reactions and conflicts," *Intl. Journal of Social Robotics*, 2022.

[7] R. Martin-Martin, M. Patel, H. Rezatofighi, A. Shenoi, J. Gwak, E. Frankel, A. Sadeghian, and S. Savarese, "Jrdb: A dataset and benchmark of egocentric robot visual perception of humans in built environments," *IEEE Transactions on Pattern Analysis and Machine Intelligence*, 2021.

[8] H. Karnan, A. Nair, X. Xiao, G. Warnell, S. Pirk, A. Toshev, J. Hart, J. Biswas, and P. Stone, "Socially compliant navigation dataset (scand): A large-scale dataset of demonstrations for social navigation," *IEEE Robotics and Automation Letters (RA-L)*, 2022.

[9] A. Wang, D. Sato, Y. Corzo, S. Simkin, A. Biswas, and A. Steinfeld, "TBD Pedestrian Data Collection: Towards Rich, Portable, and Large-Scale Natural Pedestrian Data," in *Proc. of the IEEE Intl. Conf. on Robotics & Automation (ICRA)*, IEEE, 2024.

[10] D. Helbing and P. Molnar, "Social force model for pedestrian dynamics," *Physical review E*, 1995.

[11] G. Jocher and J. Qiu, *Ultralytics yolo11*.

[12] S. Hossain, F. T. Johora, J. P. Müller, S. Hartmann, and A. Reinhardt, "SFMGNet: A physics-based neural network to predict pedestrian trajectories," *AAAI Spring Symposium on Machine Learning and Knowledge Engineering for Hybrid Intelligence*, 2022.

[13] S. Agrawal, N. Dengler, and M. Bennewitz, "Evaluating Robot Influence on Pedestrian Behavior Models for Crowd Simulation and Benchmarking," *Proc. of the Intl. Conf. on Social Robotics (ICSR)*, 2024.

[14] G. Ferrer, A. Garrell, and A. Sanfeliu, "Robot companion: A social-force based approach with human awareness-navigation in crowded environments," in *Proc. of the IEEE/RSJ Intl. Conf. on Intelligent Robots and Systems (IROS)*, 2013.

[15] G. Zhang, Z. Yu, D. Jin, and Y. Li, "Physics-infused machine learning for crowd simulation," in *Proc. of the 28th ACM SIGKDD Conference on Knowledge Discovery and Data Mining*, 2022.

[16] U. Weidmann, "Transporttechnik der fußgänger: transporttechnische eigenschaften des fußgängerverkehrs, literaturauswertung," *IVT Schriftenreihe*, 1993.

[17] E. Bosina and U. Weidmann, "Estimating pedestrian speed using aggregated literature data," *Physica A: Statistical Mechanics and its Applications*, 2017.

[18] S. B. P. Samarakoon, M. V. J. Muthugala, and A. B. P. Jayasekara, "A review on human–robot proxemics," *Electronics*, 2022.

[19] S. Pellegrini, A. Ess, K. Schindler, and L. Van Gool, "You'll never walk alone: Modeling social behavior for multi-target tracking," in *Proc. of the IEEE Intl. Conf. on Computer Vision (ICCV)*, 2009.